International Journal of Pharmaceutics 386 (2010) 249–255

Contents lists available at ScienceDirect

International Journal of Pharmaceutics

journal homepage: www.elsevier.com/locate/ijpharm

Pharmaceutical Nanotechnology

Preparation and evaluation of anti-neuroexcitation peptide (ANEP) loaded *N*-trimethyl chitosan chloride nanoparticles for brain-targeting

Siling Wang[a,*], Tongying Jiang[a], Mingxin Ma[a], Yanchen Hu[a], Jinghai Zhang[b]

[a] School of Pharmacy, Shenyang Pharmaceutical University, Wenhua Road 103, Shenyang 110016, PR China
[b] School of Pharmaceutics and Pharmaceutical Engineering, Shenyang Pharmaceutical University, Shenyang 110016, PR China

ARTICLE INFO

Article history:
Received 30 August 2009
Received in revised form 21 October 2009
Accepted 1 November 2009
Available online 10 November 2009

Keywords:
Anti-neuroexcitation peptide
Brain-targeting
N-Trimethyl chitosan chloride
Nanoparticles
Biodistribution

ABSTRACT

Anti-neuroexcitation peptide (ANEP) is a promising candidate for the treatment of neuroexcitation-associated diseases. *N*-Trimethyl chitosan (TMC) with different degrees of quaternization was synthesized, characterized and evaluated as a brain-targeting delivery vehicle for ANEP. ANEP-loaded TMC nanoparticles were prepared by ionic crosslinking of TMC with tripolyphosphate (TPP). The optimized formulation of nanoparticles consisted of TMC with a degree of quaternization (DQ) of 36.1% and TPP solution with a concentration of 0.6 mg/mL. The mean encapsulation efficiency and loading capacity of the optimum formulation was 80.63% and 185.4 μg/mL, respectively, while the mean particle size, zeta potential, and pH value were 255 nm, 32.0 mV and 6.61, respectively. ANEP was labeled with FITC for *in vivo* tissue distribution experiments. The results showed that the targetability of ANEP to brain was significantly increased by TMC nanoparticles. Absorptive-mediated transcytosis was believed to be the main pathway for the brain-targeting of FITC–ANEP–TMC/NPs. These findings demonstrate that TMC nanoparticles are potentially useful brain-targeting delivery systems for ANEP.

1. Introduction

Neuroexcitation is involved in many diseases, including epilepsy and convulsions. Epilepsy is the most common serious neurological disorder, with an incidence of 0.5–1% in the general population (McCorry et al., 2004). At present, the most widely used antiepileptic therapeutical agents clinically are chemicals and chronic toxic effects are often associated with the long-term administration of such antiepileptic drugs. As we have reported previously, anti-neuroexcitation peptide (ANEP) is a novel recombinant peptide obtained from the venom of the Chinese scorpion *Buthus martensii* Karsch, which is one of the most promising candidates for the treatment of neuroexcitation-associated diseases (Ma et al., 2007). As a potent active peptide for therapeutic use, the development of a suitable drug delivery system for ANEP is necessary. However, for the treatment of most brain disorders, delivering therapeutic agents to the brain presents a major challenge. In the central nervous system (CNS), the unique properties of the blood–brain barrier (BBB) restrict the passage of a wide variety of chemical substances and macromolecule between the systemic circulation and the neural tissue itself, while still allowing the passage of substances essential for metabolic function. The distinct anatomical features of the BBB involve the endothelial tight junctions, minimal endothelial pinocytosis, and full participation of the abluminal side of the capillary endothelium in astrocyte foot processes (Lu et al., 2005). In order to improve brain entry, many noninvasive CNS delivery techniques have been adopted. Absorptive-mediated endocytosis has been shown to be an effective process for brain drug delivery (Tsuji and Tamai, 1999; Bickel et al., 2001; Thöle et al., 2002). This kind of active brain-targeting represents a promising noninvasive strategy for facilitating drug entry into the brain.

Chitosan is a biocompatible, biodegradable and non-toxic polymer (Hirano et al., 1998; Chandy and Sharma, 1990), which has been widely used as a pharmaceutical and cosmetic excipient (Junginger and Verhoef, 1998; Kumar, 2000). However, chitosan has an apparent *pKa* of 5.5. Therefore, the polymer is only soluble in acidic conditions, where most of the amino groups are protonated. Thus, the application of chitosan is limited owing to its insolubility at physiological pH. To overcome this problem, *N*-trimethyl chitosan chloride (TMC), a partially quaternized chitosan derivative, was synthesized in this study. TMC is completely soluble in water over a wide pH range (Muzzarelli et al., 1999) and is an attractive alternative to chitosan for the preparation of protein-loaded particles by ionic crosslinking. Furthermore, the positive TMC nanoparticles can induce absorption-mediated transcytosis (AMT) triggered by an electrostatic interaction between positive nanoparticles and negatively charged plasma membranes. Many published articles have shown that positively modified nanoparticles (especially cationic bovine serum albumin-modified nanoparticles) could accumulate

* Corresponding author. Tel.: +86 24 23986348; fax: +86 24 23986348.
E-mail address: wangslsy@163.com (S. Wang).

0378-5173/$ – see front matter © 2009 Elsevier B.V. All rights reserved.
doi:10.1016/j.ijpharm.2009.11.002

in the brain (Temsamani et al., 2000; Kumagai et al., 1987). In the present study, ANEP-loaded TMC nanoparticles were prepared by an ionic crosslinking technique with tripolyphosphate (TPP) and the properties of the obtained ANEP-loaded TMC nanoparticles were investigated. In the mild ionic gelation procedure, the use of harmful organic solvents can be avoided during the preparation and loading process (Domard et al., 1986). Another objective of this work was to explore the potential of TMC nanoparticles as a brain-targeting delivery system for ANEP. The mechanism of this brain-targeting was also evaluated.

2. Materials and methods

2.1. Materials

Chitosan (85% degree of deacetylation and a molecular weight of 500 kDa) was a generous gift from Jinan Haidebei Marine Biological Product Co. Ltd. (Jinan, China). ANEP was prepared according to an improved method as we previously described (Ma et al., 2007). Fluorescein isothiocyanate (FITC) was purchased from Sigma Chem. Co. (St. Louis, MO, USA). Unless otherwise stated, all laboratory reagents were of analytical grade or better.

2.2. Methods

2.2.1. Synthesis of TMC

N-Trimethyl chitosan chloride (TMC) with different degrees of quaternization was synthesized by methylation of chitosan with iodomethane in the presence of a strong base. TMC with a generally used degree of quaternization (Amidi et al., 2006; Chen et al., 2006) was prepared by a classic two-step synthesis (Sieval et al., 1998). To synthesize TMC with a high degree of quaternization, the number of reaction steps was varied, with a modification of the methylation process from two reaction steps to one reaction step and two additional steps (Polnok et al., 2004). Briefly, a mixture of 2 g chitosan, 4.8 g sodium iodide and 11 mL 15% (w/w) aqueous NaOH in 80 mL N-methylpyrrolidinone was placed in a flask fitted with a Liebig condenser and maintained in a water bath under stirring at 60 °C for 20 min. Then, 12 mL CH_3I was added to the mixture and the reaction was continued for another 60 min. At this point, an additional step was performed involving adding 5 mL CH_3I and 10 mL 20% (w/w) NaOH. The reaction was continued for 60 min at the same temperature and then the addition was repeated and the reaction was stopped after 60 min.

The product was then precipitated from solution using ethanol and diethyl ether, and washed three times with ethanol and diethyl ether. The dried product was then dissolved in 5% (w/w) NaCl aqueous solution to allow iodide ions to exchange with chloride ions. Afterwards, the solution was desalted using a Stirred Ultrafiltration Cell (Model 8010, Millipore, USA) until no precipitation of chloride ions was detected by reaction of an aliquot of effluent with silver nitrate solution. The final polymer was obtained by freeze-drying. The purified TMC samples were analyzed by ^{1}H NMR spectroscopy (AVANCE-600, Bruker, Switzerland) with suppression of the water peak. The degree of quaternization (DQ) was calculated using the following equation (Thanou et al., 2000):

$$\mathrm{DQ} = \left[\frac{[(\mathrm{CH_3})_3]}{[\mathrm{H}]} \times \frac{1}{9}\right] \times 100\%$$

where DQ is the degree of quaternization as a percentage, $[(CH_3)_3]$ is the integral of the chemical shift of the trimethyl amino group at 3.3 ppm, and [H] is the integral of the ^{1}H peaks between 4.8 and 5.7 ppm.

The degree of substitution at the 3- and 6-hydroxyl groups of chitosan was calculated using data from the same ^{1}H NMR spectra. The chemical shifts of 3- and 6-hydroxymethyl groups were assigned as 3.5 and 3.4 ppm, respectively. The degree of O-methylation of the polymer was calculated as follows:

$$\mathrm{DOM} = \left[\frac{[(\mathrm{CH_3})_3]}{[\mathrm{H}]} \times \frac{1}{3}\right] \times 100\%$$

where DOM is the degree of O-methylation as a percentage, $[(CH_3)]$ is the integral of the chemical shift of methyl substitution for 3- or 6-hydroxyl groups at 3.5 ppm or 3.4 ppm, respectively, and [H] is the integral of the ^{1}H peaks between 4.8 and 5.7 ppm.

2.2.2. Preparation and characterizations of TMC nanoparticles

The TMC nanoparticles were prepared by the ionic gelation of TMC with TPP anions. TMC (10 mg, DQ = 36% or 86%) was dissolved in 5 mL water. Then, TPP solutions with various concentrations (from 0.5 to 1.2 mg/mL) were added dropwise to the above solution under magnetic stirring at room temperature. ANEP-loaded TMC nanoparticles were prepared as described above by dissolving different amounts (40, 80, 100, 150 or 250 μg) of ANEP in 5 mL TMC solution before adding TPP (Method A), or different amounts of ANEP were dissolved in TPP solution, and then added to TMC solution (Method B).

The loading efficiency and capacity of the protein-loaded TMC nanoparticles were determined by the following method. The free peptide was separated from the nanoparticles by centrifugation at 18,000 × *g* for 15 min. The amount of non-entrapped peptide remaining in the supernatant was measured by micro-BCA protein assay (Pierce, USA). The supernatant of non-loaded TMC nanoparticle (NP) suspension was used as a blank to correct for interference by free TMC. The loading efficiency and loading capacity of the nanoparticles were calculated as follows:

$$\text{Loading efficiency} = \frac{\text{Total amount of ANEP} - \text{free ANEP}}{\text{Total amount of ANEP}} \times 100\%$$

$$\text{Loading capacity} = \frac{\text{Total amount of ANEP} - \text{free ANEP}}{\text{Volume of NP suspension}}$$

Morphological examination of ANEP-loaded TMC nanoparticles was performed using a transmission microscope (JEM-1200EX, Japan). The size of TMC nanoparticles was measured with a Nicomp submicron particle analyzer (NICOMP 380 ZLS, Santa Barbara, CA, USA) and the zeta potential was determined using a Zeta Potential Analyzer (Delsa 440SX, Backman Coulter, USA).

2.2.3. Protein stability in the nanoparticles

The integrity of the proteins in TMC nanoparticles after ionic gelation was evaluated by SDS-polyacrylamide gel electrophoresis (SDS-PAGE). Aliquots of samples underwent electrophoresis on 15% SDS–polyacrylamide gel under reducing conditions. After electrophoresis, the protein bands were visualized by staining with coomassie brilliant blue.

2.2.4. Stability studies of nanoparticle suspensions

Nanoparticle suspensions were sealed in ampoules immediately after preparation and stored at −20 or 4 °C. The average particle size was determined by the methods described above.

2.2.5. In vivo biodistribution study

Synthesis of FITC-labeled ANEP (FITC–ANEP) and FITC-labeled TMC (FITC-TMC). In order to detect ANEP effectively *in vivo*, ANEP and TMC were labeled with FITC according to the synthetic route shown in Fig. 1. The isothiocyanate group of FITC reacted with the amino group of ANEP or TMC. Briefly, FITC was dissolved in sodium carbonate buffer (pH 9.0) and added dropwise to the ANEP or TMC solution. The reaction mixture was stirred for 8 h and then dialyzed against distilled water (MWCO 3500 or 12000). The FITC-labeled product was obtained as a fluffy sponge-like material by freeze-drying

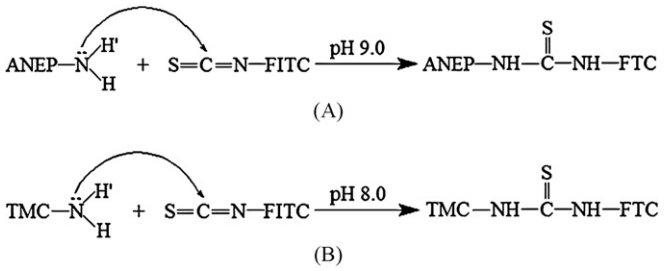

Fig. 1. Synthesis of FITC-labeled ANEP (FITC–ANEP) (A) and FITC-labeled TMC (FITC–TMC) (B).

the dialyzed solution. Fluorospectrophotometry and indirect ELISA methods were used to measure the *F/P* (FITC/peptide) value of FITC–ANEP (Ma et al., 2007). All procedures were carried out with protection from light.

Preparation of (FITC–ANEP-loaded TMC nanoparticles) and (ANEP-loaded nanoparticles prepared with FITC–TMC) FITC–ANEP–TMC/NPs and ANEP–FITC–TMC/NPs were prepared at the optimal formulation using FITC–ANEP instead of ANEP and FITC–TMC instead of TMC, respectively.

Biodistribution of FITC–ANEP-loaded TMC nanoparticles Male KunMing mice (18–22 g) were purchased from the Experimental Animal Center of Shenyang Pharmaceutical University (Shenyang, China). All experimental procedures carried out in this study were performed in accordance with the Guidelines for the Care and Use of Laboratory Animals of Shenyang Pharmaceutical University. Mice were injected with FITC–ANEP–TMC/NPs or FITC–ANEP solution via the tail vein, both at a dose of 3 mg/kg, after fasting for 12 h. At different intervals, immediately after blood depletion, the brains, hearts, livers, spleens, lungs and kidneys were removed and washed with saline, adhering tissues/fluids were removed and the organs were weighed after the mice were killed. The fluorescence intensity in the different tissues was measured at λ_{ex} 485 and λ_{em} 535 nm with a 1420 Multilabel Counter (PerkinElmer Singapore Pte Ltd.).

The targetability was also calculated from the following equation:

$$C_e = \frac{C_{max,NPs}}{C_{max,solutions}}$$

where $C_{max,NPs}$ is the peak concentration of the drug in various tissues of the FITC–ANEP–TMC/NP group, and $C_{max,solution}$ is that of the FITC–ANEP solution group.

2.2.6. Investigation of the mechanism of brain-targeting of TMC nanoparticles

Four groups were used in this study: FITC–ANEP solution, FITC solution, FITC–ANEP–TMC/NPs and ANEP–FITC–TMC/NPs. The injected dose of the peptide in all groups was 3.0 mg/kg. For the FITC solution group, the injected dose of FITC was 24 μg/kg, which gave the same fluorescence intensity as FITC–ANEP. The brain biodistribution experiments were carried on according to the above-mentioned protocols. At different intervals, immediately after blood depletion, the brains were removed and washed with saline, adhering tissues/fluids were removed, and the organs were weighed. The fluorescence intensity in different tissues was measured at λ_{ex} 485 and λ_{em} 535 nm.

2.2.7. Statistical analysis

All data are reported as mean ± standard error of the mean. The differences between the groups were examined using Student's *t*-test. *P*-values less than 0.05 were considered statistically significant.

Table 1
Peak assignment of ^{1}H NMR spectra of TMC.

δ (ppm)	3.3	3.1	2.1	3.5	3.4
Peak ascription	$-N^+(C\underline{H}_3)_3$	$-N(C\underline{H}_3)_2$	$-NHCOC\underline{H}_3$	$3\text{-}OC\underline{H}_3$	$6\text{-}OC\underline{H}_3$

Table 2
Degree of quaternization and O-methylation of the TMC polymers.

TMC polymer	DQ (%)	3-OCH_3 (%)	6-OCH_3 (%)
TMC36	36	15.6	68.7
TMC86	86	61.6	43.1

3. Results and discussion

3.1. TMC synthesis and characterization by NMR spectroscopy

TMC polymers with low and high degrees of quaternization were synthesized by varying the number of reaction steps. The yields were 25% and 30%, respectively, calculated by the ratio of the weight of purified lyophilized trimethylated product to the weight of the initial chitosan. According to the related reference (Hamman and Kotze, 2001), the peaks of the synthesized TMC obtained from ^{1}H NMR spectra are shown in Table 1. The calculated degrees of quaternization and O-methylation of the two TMC polymers are summarized in Table 2. The degree of quaternization increased significantly with the additional reaction steps. The results of the solubility experiment showed that the solubility of TMC in both solvents was more than 2%. Unlike chitosan, the synthetic TMC could be dissolved in both water and pH 7.4 PBS.

3.2. Preparation and characterization of TMC nanoparticles

The TMC nanoparticles were prepared by ionic gelation. This mild technique involves the mixing of two aqueous solutions at ambient temperature without sonication or using organic solvents (Van Der Lubben et al., 2001). Since proteins and peptides are very labile molecules and sensitive to several stress factors, this mild preparation method is very suitable for the preparation of peptide-loaded nanoparticles.

3.2.1. Effect of preparation methods of TMC nanoparticles

The loading efficiency of ANEP-loaded nanoparticles (TMC 2 mg/mL, ANEP 0.5 mg) obtained by method A and B is 72% and 79%, respectively. Compared with method A, method B improved the loading efficiency. When ANEP was added to TPP solution in method B, ANEP (p*I* = 5.2) had a negative charge before it was added to TMC solution. Consequently, the ionic interaction and ionic crosslinking between negatively charged ANEP and positively charged TMC were more intense, leading to higher loading efficiency.

3.2.2. Effect of TMC/TPP (w/w) ratio

Three different phenomena could be observed during the preparation process: solution, opalescent suspension and aggregation. As was shown in Table 3, the particle size became smaller and the loading efficiency increased as the amount of TPP increased. In the

Table 3
Effect of TMC/TPP (w/w) ratio on the characteristics of prepared TMC nanoparticles (TMC 2 mg/ml, ANEP 0.5 mg) (n = 3).

TMC/TPP ratio (w/w)	Particle size (nm) (mean ± SD)	Loading efficiency (%) (mean ± SD)
6.2	369 ± 20	63.51 ± 3.10
5.2	327 ± 19	74.20 ± 2.91
4.5	254 ± 13	79.89 ± 1.71

Table 4
Loading efficiency, loading capacity and particle size of ANEP-loaded TMC nanoparticles prepared with different concentrations of TPP (TMC 2 mg/mL, ANEP 0.5 mg) ($n = 3$).

TPP concentration (mg/ml)	Loading efficiency (%) (mean ± SD)	Loading capacity (μg/ml) (mean ± SD)	Particle size (nm) (mean ± SD)
0.400	80.45 ± 2.67	38.09 ± 1.34	312 ± 23
0.600	79.90 ± 1.59	45.92 ± 0.91	257 ± 11
0.800	60.83 ± 1.64	41.78 ± 1.05	273 ± 13
1.000	39.11 ± 1.87	27.08 ± 1.30	268 ± 14
1.200	41.45 ± 2.75	30.26 ± 2.01	301 ± 23

Table 5
Effect of ANEP concentrations on loading efficiency, loading capacity and particle size of ANEP-loaded TMC nanoparticles ($n = 3$).

Added ANEP (mg)	Loading efficiency (%) (mean ± SD)	Loading capacity (μg/ml) (mean ± SD)	Particle size (nm) (mean ± SD)
0.2	73.81 ± 2.73	16.97 ± 0.63	254 ± 15
0.5	79.65 ± 1.86	45.78 ± 1.07	259 ± 14
1.0	79.76 ± 1.73	91.68 ± 1.99	255 ± 16
1.5	80.82 ± 2.06	139.3 ± 3.55	266 ± 13
2.0	80.88 ± 2.29	186.0 ± 5.26	262 ± 15

successive study, TMC nanoparticles with an obvious opalescence were prepared and the TMC/TPP (w/w) ratio was about 4.5, and so consistent with the optimal ratio of 3–5 for chitosan/TPP (w/w) found by Calvo et al. (1997a,b). At extremely high or low TMC/TPP ratios, either a clear solution (almost no particle formation) or a larger nanoparticle aggregation with a low stability was obtained (Gan et al., 2005).

3.2.3. *Effect of TPP and protein concentrations on loading efficiency and loading capacity of TMC nanoparticles*

Several formulations were prepared with TPP solutions with different initial concentrations (0.4–1.2 mg/mL) to establish the preparation conditions under which nanoparticles could be formed. As can be seen from Table 4, TMC nanoparticles have higher loading efficiency and loading capacity when the concentration of TPP is selected as 0.6 mg/mL. Table 5 shows the effect of the protein concentration on the loading efficiency and loading capacity of TMC nanoparticles. When the amount of added ANEP increased from 0.2 to 2.0 mg, the loading efficiency of ANEP increased from 74% to 81% and the loading capacity increased from 17 to 186 μg/mL. The high loading efficiency for ANEP is likely due to electrostatic interactions between the positively charged TMC and negatively charged ANEP (pI = 5.2). Table 5 also shows that the ANEP concentration had an obvious effect on the particle size of the nanoparticles.

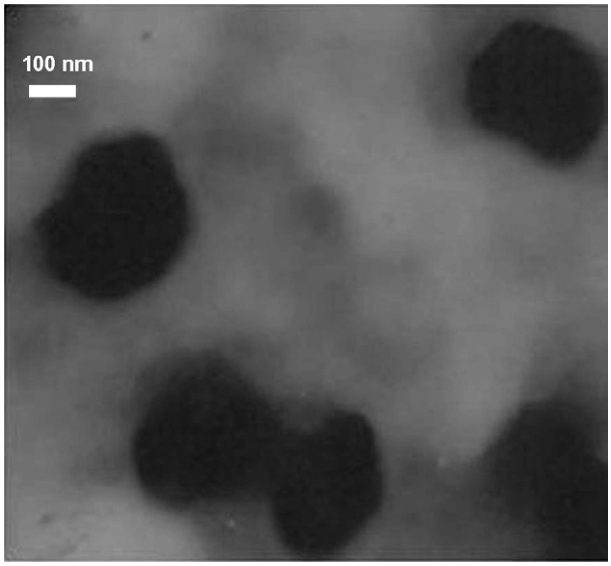

Fig. 2. TEM photograph of ANEP–TMC/NPs.

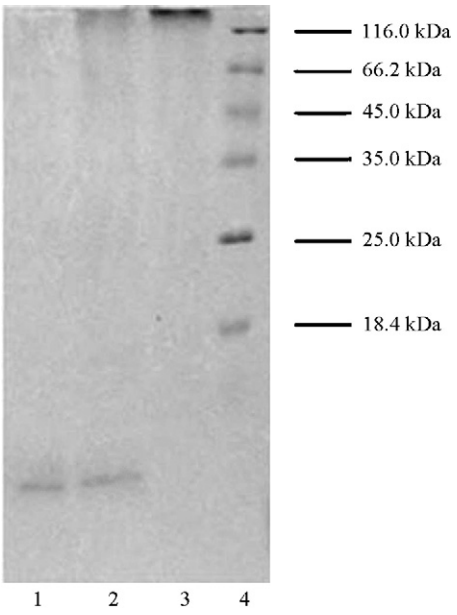

Fig. 3. SDS-PAGE under reducing conditions. Lane 1: free ANEP in PBS; lane 2: ANEP–TMC/NPs; lane 3: empty TMC nanoparticles; lane 4: molecular weight markers.

3.2.4. *Effect of degree of quaternization of TMC on the physicochemical properties of TMC nanoparticles*

As was shown in Table 6, the loading efficiency of ANEP was increased with a lower degree of quaternization. A similar phenomenon was observed in studies on bovine hemoglobin-loaded TMC nanoparticles (Chen et al., 2006). Both types of nanoparticles prepared using the two kinds of TMC had a narrow size distribution and a positive surface charge. Nanoparticles prepared by TMC with a high degree of quaternization had a larger particle size and higher zeta potential. This may be due to the higher positive charge of TMC86 than TMC36 attributing to the higher degree of quaternization. The net charge carried by TMC86 nanoparticles was more than that by TMC36 nanoparticles, although the difference was not significant ($P > 0.05$).

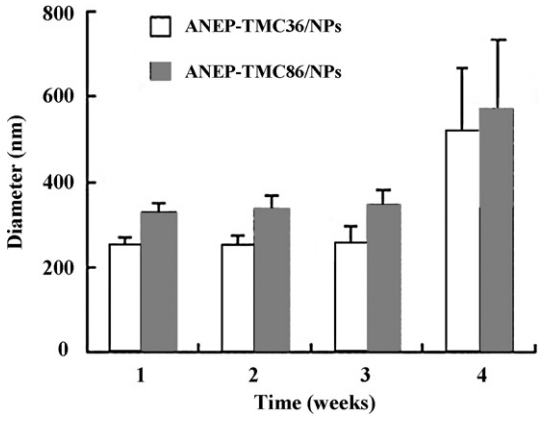

Fig. 4. Average particle size of ANEP–TMC nanoparticles as a function of time. Each point represents the mean diameter ± distribution.

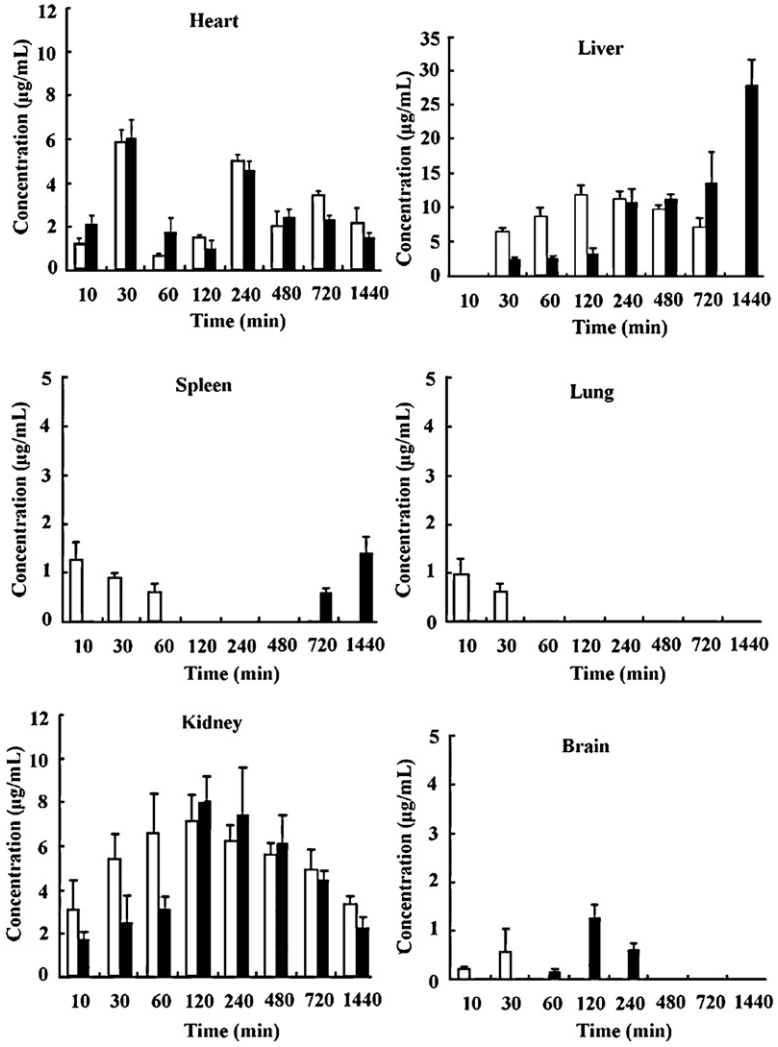

Fig. 5. The FITC–ANEP concentration at different times in different tissues after injecting FITC–ANEP–TMC/NPs (black stands) and FITC–ANEP solution (white stands) intravenously. Each point represents the mean concentration ± SD, $n = 6$.

Table 6
The influence of DQ on the characteristics of ANEP-loaded TMC nanoparticles ($n = 3$).

DQ of TMC polymers (%)	Loading efficiency (%) (mean ± SD)	Loading capacity (μg/ml) (mean ± SD)	Particle size (nm) (mean ± SD)	Zeta potential (mV) (mean ± SD)
36	80.63 ± 2.36	185.4 ± 5.4	255 ± 11	32.0 ± 2.12
86	76.12 ± 2.33	175.0 ± 5.4	339 ± 21	38.8 ± 1.42

3.2.5. Morphology of nanoparticles

The transmission electron photomicrograms of ANEP-loaded TMC nanoparticles are shown in Fig. 2. All nanoparticles were found to be nearly spherical in shape.

3.3. Stability

3.3.1. Protein stability in the preparation process

The SDS-PAGE measurement showed that ANEP remained stable after being formulated in nanoparticles. No additional bands indicating the presence of aggregates or fragments were visible (Fig. 3). This shows that the ionic gelation method is mild enough to protect the peptide during the preparation procedure.

3.3.2. Stability of nanoparticle suspensions

When frozen nanoparticle suspensions thawed out, aggregation was clearly observed. Thus, it is not suitable to store them at −20 °C. The changes in particle size at 4 °C during a storage period of 4 weeks are shown in Fig. 4. When stored at 4 °C, the nanoparticle suspensions were stable for 3 weeks and the particle size dramatically increased after 4 weeks. Freeze-drying technology was investigated to solve the problem of the stability of nanoparticles in subsequent studies (data not shown).

3.4. In vivo study

The determined *F*/*P* ratio of the FITC–ANEP conjugate was 7.86 ng/μg. The characteristics of the prepared

Table 7
C_e value of FITC–ANEP–TMC/NPs in tissues compared with FITC–ANEP solution.

Tissue	Heart	Liver	Spleen	Lung	Kidney	Brain
$C_{max,NPs}$	6.012	27.981	1.404	0	8.343	1.306
$C_{max,solution}$	5.830	11.759	1.275	0.978	7.429	0.584
C_e	1.031	2.380	1.101	0	1.123	2.236

Table 8
FITC concentration in brain after i.v. administration of FITC solution, FITC, FITC–ANEP–TMC/NPs and ANEP–FITC–TMC/NPs (ND means not determined).

Time (min)	Concentration of FITC (ng/ml)			
	FITC solution	FITC	FITC–ANEP–TMC/NPs	ANEP–FITC–TMC/NPs
10	1.719 ± 0.626	ND	ND	ND
30	4.590 ± 0.466	ND	ND	4.018 ± 1.067
60	ND	ND	1.485 ± 0.185	5.665 ± 0.992
120	ND	ND	10.269 ± 2.129	6.912 ± 0.323
240	ND	3.286 ± 0.794	4.933 ± 0.136	5.202 ± 2.345
480	ND	2.022 ± 0.709	ND	7.101 ± 2.749
720	ND	1.505 ± 0.532	ND	2.371 ± 0.882
1440	ND	ND	ND	ND

FITC–ANEP–TMC/NPs were similar to those of ANEP-loaded TMC nanoparticles. The results of the tissue distribution of the FITC–ANEP–TMC/NPs group and FITC–ANEP solution group after i.v. injection are shown in Fig. 5. For both groups, the peptide was mainly distributed in liver, heart and kidney. In brain, the ANEP was distributed rapidly and transiently and the maximum concentration appeared at 30 min after administration of FITC–ANEP solution, which was consistent with the report of the onset time of ANEP (Zhang et al., 2001). As for animals in the FITC–ANEP–TMC/NPs group, ANEP appeared in the brain 1 h after injection and remained there for 3 h.

The C_e values are shown in Table 7. The C_e value of brain was 2.236. This indicated that the affinity for brain was significantly increased by FITC–ANEP–TMC/NPs compared with FITC–ANEP solution ($P<0.01$). A high C_e value was also observed in liver. The C_e values for the heart, spleen and kidney were all close to 1.0 and there were no significant biodistribution differences between the two groups as far as these tissues were concerned. The C_e value of lung was zero, which means that the nanoparticles underwent very little distribution into lung.

To investigate the mechanism of brain-targeting, ANEP and TMC were labeled with FITC and were used to prepare nanoparticles. The brain biodistribution of the four groups is shown in Table 8 and Fig. 6. For the simple FITC solution, very little was observed in brain which indicated there was no interference from false positive results. The group of ANEP–FITC–TMC/NPs exhibited strong fluorescence in brain and the brain biodistribution was consistent with the results obtained in the group of FITC–ANEP–TMC/NPs, which indicated that NPs could be transported across the BBB. Absorption-mediated transcytosis is supposed to be the main pathway for the phenomenon of brain-targeting exhibited by FITC–ANEP–TMC/NPs. From the above-described results, the nanoparticles have a positive zeta potential of 30.7 mV. Absorption-mediated transcytosis (AMT) is triggered by an electrostatic interaction between the positively charged moiety of the nanoparticles and a negatively charged plasma membrane surface region on the brain capillary endothelium. Fluorescent micrographs also showed the corresponding brain biodistribution results in the four groups. Similar to the results obtained in our studies, Huang et al. (Huang et al., 2004) proved that the uptake of chitosan nanoparticles by A549 cells was initiated by electrostatic interactions between the nanoparticles and the cell membrane; Amidi et al. found that FITC–albumin-associated TMC nanoparticles could be transported across the nasal mucosa due to intracellular uptake by epithelial and NALT cells in a series of in vivo uptake studies (Amidi et al., 2007). The role of TMC nanoparticles as brain-targeting carriers is reported here for the first time.

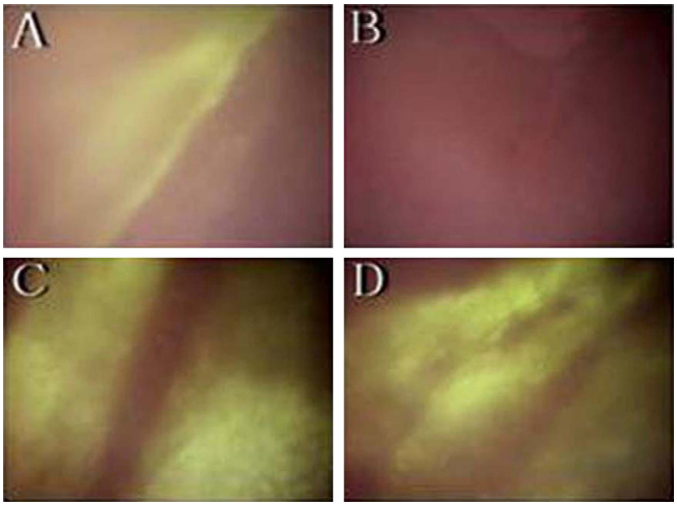

Fig. 6. Fluorescent micrographs of frozen mouse brain sections after the i.v. administration of (A) FITC–ANEP solution at 2 h; (B) FITC at 30 min; (C) FITC–ANEP–TMC/NPs at 2 h and (D) ANEP–FITC–TMC/NPs at 2 h (400×).

4. Conclusions

In order to develop a novel brain-targeting delivery system for ANEP, a water-soluble cationic chitosan derivative, *N*-trimethyl chitosan chloride (TMC), was synthesized, characterized and used as a vehicle. Under optimal conditions, ANEP was successfully incorporated into TMC nanoparticles by mild ionic crosslinking with TPP. The physicochemical characteristics and stability of the nanoparticles were investigated. Furthermore, TMC nanoparticles significantly enhanced the biodistribution of ANEP in brain through absorption-mediated transcytosis. These results suggest that TMC nanoparticles offer an effective and promising brain-targeting delivery system, especially for peptides or proteins.

Acknowledgements

This work was supported by the National Basic Research Program of China (973 Program, 2009CB930300) and National Natural Science Foundation of China (30901864).

References

Amidi, M., Romeijn, S.G., Borchard, G., Junginge, H.E., Hennink, W.E., Jiskoot, W., 2006. Preparation and characterization of protein-loaded N-trimethyl chitosan nanoparticles as nasal delivery system. J. Control. Release 111, 107–116.
Amidi, M., Romeijn, S.G., Verhoef, J.C., Junginger, H.E., Bungener, L., Huckriede, A., Crommelin, D.J.A., Jiskoot, W., 2007. N-Trimethyl chitosan (TMC) nanoparticles loaded with influenza subunit antigen for intranasal vaccination: biological properties and immunogenicity in a mouse model. Vaccine 25, 144–153.
Bickel, U., Yoshikawa, T., Pardridge, W.M., 2001. Delivery of peptides and proteins through the blood–brain barrier. Adv. Drug Deliv. Rev. 46, 247–279.
Calvo, P., Remunan-Lopez, C., Vila-Jato, J.L., Alonso, M.J., 1997a. Novel hydrophilic chitosan polyethylene oxide nanoparticles as protein carriers. J. Appl. Polym. Sci. 63, 125–132.
Calvo, P., Remunan-Lopez, C., Vila-Jato, J.L., Alonso, M.J., 1997b. Chitosan and chitosan/ethylene oxide-propylene oxide block copolymer nanoparticles as novel carriers for proteins and vaccines. Pharm. Res. 14, 1431–1436.
Chandy, T., Sharma, C.P., 1990. Chitosan as a biomaterial. Biomat. Art. Cells Art. Org. 18, 1–24.

Chen, F., Zhang, Z.R., Huang, Y., 2006. Evaluation and modification of *N*-trimethyl chitosan chloride nanoparticles as protein carriers. Int. J. Pharm. 336, 166–173.
Domard, A., Rinaudo, M., Terrassin, C., 1986. New method for the quaternization of chitosan. Int. J. Biol. Macromol. 8, 105–107.
Gan, Q., Wang, T., Cochrane, C., McCarron, P., 2005. Modulation of surface charge, particle size and morphological properties of chitosan-TPP nanoparticles intended for gene delivery. Colloids Surf. B: Biointerfaces 44, 65–73.
Hamman, J.H., Kotze, A.F., 2001. Effect of the type of base and number of reaction steps on the degree of quaternization and molecular weight of N-trimethyl chitosan chloride. Drug Dev. Ind. Pharm. 27, 373–380.
Hirano, S., Seino, H., Akiyama, Y., Nonaka, I., 1998. Biocompatibiity of chitosan by oral and intravenous administration. Polym. Eng. Sci. 59, 897–901.
Huang, M., Khor, E., Lim, L.Y., 2004. Uptake and cytotoxicity of chitosan molecules and nanoparticles: effects of molecular weight and degree of deacetylation. Pharm. Res. 21, 344–353.
Junginger, H.E., Verhoef, J.C., 1998. Macromolecules as safe penetration enhancers for hydrophilic drugs—a fiction? Pharm. Sci. Technol. Today 1, 370–376.
Kumagai, A.K., Eisenberg, J.B., Pardridge, W.M., 1987. Absorptive-mediated endocytosis of cationized albumin and a beta-endorphin-cationized albumin chimeric peptide by isolated brain capillaries. Model system of blood–brain barrier transport. J. Biol. Chem. 262, 15214–15219.
Kumar, M.N.V.R., 2000. A review of chitin and chitosan applications. React. Funct. Polym. 46, 1–27.
Lu, W., Tan, Y.Z., Hu, K.L., Jiang, X.G., 2005. Cationic albumin conjugated pegylated nanoparticle with its transcytosis ability and little toxicity against blood–brain barrier. Int. J. Pharm. 295, 247–260.
Ma, M., Zhang, J., Li, W., Liu, Y.F., Wang, S.L., 2007. Development of an improved preparation and an enzyme-linked immunosorbent assay for antineuroexcitation peptide (ANEP). J. Biochem. Biophys. Methods 70, 635–640.
McCorry, D., Chadwick, D., Marson, A., 2004. Current drug treatment of epilepsy in adults. Lancet Neurol. 3, 729–735.
Muzzarelli, R.A., Mattioli-Belmonte, M., Pugnaloni, A., Biagini, G., 1999. Biochemistry, histology and clinical uses of chitins and chitosans in wound healing. Experientia 87, 251–264.
Polnok, A., Borchard, G., Verhoef, J.C., Sarisuta, N., Junginger, H.E., 2004. Influence of methylation process on the degree of quaternization of *N*-trimethyl chitosan chloride. Eur. J. Pharm. Biopharm. 57, 77–83.
Sieval, A.B., Thanou, M., Kotzé, A.F., Verhoef, J.C., Brussee, J., Junginger, H.E., 1998. Preparation and NMR characterization of highly substituted N-trimethyl chitosan chloride. Carbohydr. Polym. 36, 157–165.
Temsamani, J., Scherrmann, J.M., Rees, A.R., 2000. Brain drug delivery technologies: novel approaches for transporting therapeutics. Pharm. Sci. Technol. Today 3, 155–162.
Thanou, M.M., Kotzé, A.F., Scharringhausen, T., Lueβen, H.L., de Boer, A.G., Verhoef, J.C., Junginger, H.E., 2000. Effect of degree of quaternization of N-trimethyl chitosan chloride for enhanced transport of hydrophilic compounds across intestinal Caco-2 cell monolayers. J. Control. Release 64, 15–25.
Thöle, M., Nobmann, S., Huwyler, J., Bartmann, A., Fricker, G., 2002. Uptake of cationized albumin coupled liposomes by cultured porcine brain microvessel endothelial cells and intact brain capillaries. J. Drug Target. 10, 337–344.
Tsuji, A., Tamai, I., 1999. Carrier-mediated or specialized transport of drugs across the blood–brain barrier. Adv. Drug Deliv. Rev. 36, 277–290.
Van Der Lubben, I.M., Verhoef, J.C., Borchard, G., Ejunginger, H., 2001. Chitosan for mucosal vaccination. Adv. Drug Deliv. Rev. 52, 139–144.
Zhang, J.H., Hua, Z.C., Xu, Z., Zheng, W.J., Zhu, D.X., 2001. Expression of antineuroexcitation peptide (ANEP) of scorpion *Buthus martensii* Karsch in *Escherichia coli*. Prep. Biochem. Biotechnol. 31, 49–57.